

Altitude-Adjusted Corrected Geomagnetic Coordinates: Definition and Functional Approximations

S. G. Shepherd

Thayer School of Engineering, Dartmouth College, Hanover, New Hampshire, USA

Abstract. Analysis of the functional approximations used to transform between geographic and Altitude-Adjusted Corrected Geomagnetic (AACGM) coordinates reveals that errors of >50 km can occur in the auroral and polar regions. These errors are the result of efforts to better approximate AACGM coordinates near the magnetic equator and the South Atlantic Anomaly. In these regions AACGM coordinates are not defined and alternate coordinates have been used. This augmentation and emphasis on the solution in regions near the equator result in spherical harmonic approximating functions that are less accurate than need be in the auroral and polar regions. In response, a new set of spherical harmonic coefficients have been derived that better represent AACGM coordinates in these regions. These new AACGM coefficients are limited to below 2000 km in altitude in order to ensure accuracy. For altitudes above 2000 km, a magnetic field-line tracing solution is recommended. A software package developed to take advantage of the new AACGM coefficients provides the capability of tracing magnetic field lines at any altitude, for improved accuracy. In addition, linear interpolation between 5-year epochs is used to produce coordinates that vary smoothly over the entire period from 1965–present. The intent of this work is to provide a more accurate procedure for determining AACGM coordinates in the auroral and polar regions for the study of magnetospheric and ionospheric processes.

1. Introduction

Altitude-Adjusted Corrected Geomagnetic (AACGM) coordinates were originally developed for the purpose of comparing ground-based radar backscatter measurements from locations in both hemispheres. As part of the Polar Anglo-American Conjugate Experiment (PACE) a new coordinate system was developed in order to better compare measurements from two coherent backscatter radars located in Goose Bay, Labrador and Halley Bay, Antarctica [Baker and Wing, 1989]. The coordinate system, originally called the PACE geomagnetic (PGM) coordinate system but later referred to as AACGM, has been used to map numerous ground-based and space-based measurements into magnetic coordinates for studies of plasma and electromagnetic processes that span the thermosphere to the magnetosphere. Examples include ground-based radar observations of plasma convection [Greenwald *et al.*, 1990; Hanuise *et al.*, 1993; Ruohoniemi and Baker, 1998; Cousins and Shepherd, 2010], magnetospheric pulsations [Ruohoniemi *et al.*, 1991; Samson *et al.*, 1992], plasma density structures [Doe *et al.*, 1993; Rodger *et al.*, 1994]; ground-based magnetometer, riometer, and optical measurements associated with ionospheric and magnetospheric processes [Samson *et al.*, 1991; Rosenberg *et al.*, 1993; Rostoker *et al.*, 1995; Lühr *et al.*, 1998]; and satellite measurements of particles and electric currents to determine magnetospheric boundaries and large-scale structures [Newell *et al.*, 1991a, b; Sotirelis *et al.*, 1998; Watanabe *et al.*, 1998; Waters *et al.*, 2001; Korth *et al.*, 2010].

In practice, the coefficients of an expansion of spherical harmonic functions are used to obtain AACGM coordinates (and their inverse) for a given location, specified by its geographic coordinates and altitude above the surface of the

Earth. These coefficients, while providing a smooth and continuous functional description of AACGM coordinates, are in reality an approximation to the actual AACGM coordinates. AACGM coordinates and the related corrected geomagnetic (CGM) coordinates [Gustafsson, 1984; Gustafsson *et al.*, 1992] are, in fact, undefined and discontinuous in certain regions near the equator, which causes difficulties in obtaining an accurate solution. The expansion of spherical harmonic functions provides a global solution for the mapping between geographic and AACGM coordinates, but the degree to which the functional solution agrees with the underlying data varies significantly over the globe.

Several developments related to AACGM coordinates have been described in technical reports [Bhavnani and Hein, 1994; Hein and Bhavnani, 1996; Heres and Bonito, 2007]. These developments have been focused primarily on obtaining a functional approximation in the form of an expansion of spherical harmonic functions (hereafter referred to as the AACGM coefficients, or simply the coefficients) with improved accuracy near the South Atlantic Anomaly (SAA) and in the region near the magnetic equator where AACGM coordinates are undefined. In addition, the altitude range over which the coefficients are valid was extended from 600 km to 7200 km.

Since the original definition by Baker and Wing [1989] new sets of coefficients have been determined using one of the techniques described by Bhavnani and Hein [1994]; Hein and Bhavnani [1996]; Heres and Bonito [2007]. Each set of coefficients is valid for the 5-year epoch of the corresponding International Geomagnetic Reference Field (IGRF) model [c.f., Finlay *et al.*, 2010]. Complete sets of AACGM coefficients currently exist for the epochs from 1975 to 2010. These coefficients, together with software historically provided by members of the Super Dual Auroral Radar Network (SuperDARN) community, are used to map ground and space-based measurements to and from AACGM coordinates.

Comparison of the results obtained from using the existing sets of AACGM coefficients in mapping coordinates

with those obtained by performing the AACGM mapping as originally described by *Baker and Wing* [1989], reveal some inconsistencies in the coefficients derived for various epochs, suggesting that different techniques have been used. More importantly, it is apparent that emphasis on the equatorial region and higher altitudes have had the unintended consequence of reducing the accuracy of AACGM coordinates obtained from the coefficients at lower altitudes in regions of middle to polar latitudes, particularly in the SAA sector.

Several questions regarding AACGM coordinates come to mind, most importantly whether the AACGM coefficients are themselves the coordinate system (as they seem to have become) or whether they are just a useful approximation of the underlying coordinate system, which requires a numerical procedure to follow magnetic field lines in the IGRF model. Other issues include whether an official and definitive set of AACGM coefficients exists and whether they should be re-derived in entirety when developments to the technique are made.

The author takes the position that AACGM coordinates are defined by following magnetic field lines and that coefficients should be defined in a consistent and clear fashion to best approximate the AACGM coordinates. The purpose of this paper is to illustrate perceived weaknesses of the current AACGM coefficients in representing the actual AACGM coordinates at middle to polar latitudes. In addition, a technique is described that is used to obtain a new set of coefficients that represent the AACGM coordinates to a much better degree of accuracy in this region. In order to maintain a suitable degree of accuracy for altitudes extending to the upper end of low Earth orbit (LEO), the altitude range of these new coefficients is limited to 2000 km. Above this altitude it is recommended that the slower, but more accurate, field-line tracing is used. The option to perform field-line tracing at any altitude is included in a software package available from the author's web site (<http://engineering.dartmouth.edu/superdarn/aacgm.html>).

The organization of the remainder of the paper is as follows: A brief description of the AACGM coordinate system and history of developments is given in section 2. Section 3 describes the functional approximation and associated errors of the conversion from geographic to AACGM coordinates. The new AACGM approximating coefficients are introduced and discussed in section 4. Approximations associated with altitude dependence and the inverse transformation from AACGM to geographic are described in sections 5 and 6, respectively. A brief discussion of the coordinate transformations is given in section 7 followed by a summary in section 8.

2. AACGM Coordinate System

The AACGM coordinates of a given point, specified by its geographic latitude (λ_g), longitude (ϕ_g) and altitude (h) above the surface of the Earth, are determined by following the magnetic field line from the geographic starting point to the magnetic dipole equator. The AACGM coordinates are then given by the latitude and longitude of the dipole field line that connects the point on the magnetic equator to the surface of the Earth.

In practice, magnetic field lines are determined numerically from the appropriate IGRF magnetic field model. The magnetic field line is followed (or numerically traced) from the starting position to the magnetic dipole equator; defined by the best-fit, Earth-centered dipole [c.f., *Gustafsson et al.*, 1992]. The AACGM latitude (λ_m) and longitude (ϕ_m) are then simply given by the latitude and longitude of the dipole magnetic field line that connects this point with the surface of the Earth. The dipole latitude can be determined from

the L -shell of the intersection point on the magnetic equator, given by

$$\cos \lambda_m = L^{-\frac{1}{2}} \quad (1)$$

Using this technique, all points on a given field line are magnetically connected and have the same AACGM coordinates.

Figure 1 illustrates the procedure for determining AACGM coordinates (identical to CGM coordinates in this case because the starting altitude is 0 km) for four different locations on the geographic prime meridian (0° longitude.) Three red lines represent the IGRF magnetic field lines emanating from the starting locations at 50° , 40° and 30° latitude. These field lines are followed to the magnetic dipole equator, shown as a radial wireframe. The AACGM coordinates of these points are given by the dipole coordinates of the intersection point and shown by the green dipole field lines.

Using this definition of AACGM coordinates, some geographic coordinates can be seen to have no corresponding AACGM coordinate. In Figure 1, the IGRF field line emanating from the geographic location on the prime meridian and 20° latitude (magenta line) intersects Earth's surface before it reaches the magnetic dipole equator. For this reason the AACGM coordinates of this location are undefined. An entire region around the IGRF magnetic dipole equator (shown as an orange line) falls into this category. The boundary of this region is shown in Figure 1 by solid yellow lines on the Earth. In this region, the magnetic dip equator is offset from the dipole equator and IGRF field lines intersect the dipole equator below Earth's surface. The region where AACGM coordinates are undefined is referred to as the undefined region or the forbidden region [c.f., *Gustafsson et al.*, 1992].

AACGM coordinates are typically determined using this technique for each location on a regular, geographic grid. The resulting data are in some cases tabulated [*Gustafsson*, 1984; *Gustafsson et al.*, 1992] but more often are approximated by fitting an expansion of spherical harmonic functions to the tabulated data [*Baker and Wing*, 1989; *Bhavnani and Hein*, 1994; *Hein and Bhavnani*, 1996; *Heres and*

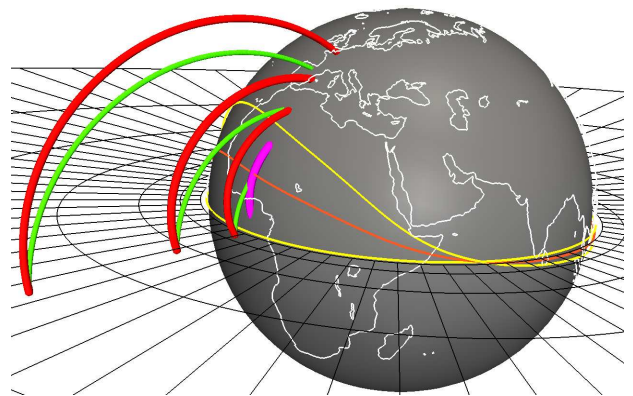


Figure 1. Examples of determining AACGM coordinates for four geographic locations along the prime meridian. Red lines represent IGRF field lines emanating from geographic starting locations at 50° , 40° , 30° latitude, and ending at the Earth-centered magnetic dipole equator. AACGM coordinates are given by the coordinates dipole field lines, shown in green. The magenta line shows the IGRF field line starting at 20° latitude, which intersects the surface of Earth before the dipole equator. AACGM coordinates are undefined for such locations. The region near the magnetic dip equator (orange line) which includes these field lines is marked by yellow lines on Earth's surface.

Bonito, 2007]. Following *Baker and Wing* [1989], the fitting is done in rectangular Cartesian coordinates (x_m, y_m, z_m) to avoid numerical singularities associated with spherical polar coordinates. The expansions are given by

$$\begin{aligned} x_m &= \sum_{l=0}^N \sum_{m=-l}^l A_{lm}^x Y_{lm}(\theta_g, \phi_g) \\ y_m &= \sum_{l=0}^N \sum_{m=-l}^l A_{lm}^y Y_{lm}(\theta_g, \phi_g) \\ z_m &= \sum_{l=0}^N \sum_{m=-l}^l A_{lm}^z Y_{lm}(\theta_g, \phi_g) \end{aligned} \quad (2)$$

where the $Y_{lm}(\theta_g, \phi_g)$ are the standard, real spherical harmonic functions and N is the order of the expansion. The AACGM colatitude (θ_m) and longitude (ϕ_m) are then given by

$$\begin{aligned} \cos \theta_m &= z_m \\ \tan \phi_m &= y_m/x_m \end{aligned} \quad (3)$$

Although *Baker and Wing* [1989] use 4th order expansions, subsequent authors use 10th order expansions for equation 2. Note that all of the currently available AACGM coefficients $\{A_{lm}^x, A_{lm}^y, A_{lm}^z\}$ are for 10th order expansions. These coefficients are then used to evaluate equations 2 and 3 for arbitrary geographic positions (θ_g, ϕ_g) .

In order to obtain a useful approximation over a range of altitudes, this procedure is performed at a series of discrete reference altitudes, where the starting location is specified by the height h above the surface of the Earth. A set of $(N+1)^2$ coefficients are obtained for each Cartesian coordinate (x_m, y_m, z_m) at each reference altitude. It is possible to use one of these sets of coefficients for a given altitude. However, if the desired altitude is not one of the reference altitudes, some form of interpolation or approximation must be used. In practice, each of the $3(N+1)^2$ coefficients are approximated using the corresponding set of values determined at the reference altitudes.

Several possible approximation schemes have been used. *Baker and Wing* [1989] derive coefficients at reference altitudes corresponding to 0, 150, 300, 450 km and simply state that interpolation may be used for altitudes up to 600 km, which suggests that a polynomial (interpolating or fit) is used to extend the altitude range beyond 450 km. Alternatively, *Bhavnani and Hein* [1994] derive coefficients at 0, 300 and 1200 km, fit a quadratic polynomial to the coefficients and extrapolation to altitudes up to 2000 km is deemed safe. Finally, *Hein and Bhavnani* [1996]; *Heres and Bonito* [2007] extend the altitude range to 7200 km by fitting a 4th order polynomial to coefficients derived at more than 20 different reference altitudes. Reference altitudes are weighted in such a way as to only allow for small deviations at 0 km altitude and to improve the fit in the 0–1200 km region.

Although some specific details of these altitude-dependent schemes are not known, it is important to note that they amount to yet another form of approximation to the AACGM coordinates. Specifics of the altitude fitting are discussed in more detail in section 5. In addition, the inverse transformation (AACGM to geographic) and a few other details related to spherical harmonic function expansions are also discussed in later sections. However, the accuracy to which the current AACGM coefficients represent AACGM coordinates is first investigated.

3. AACGM Functional Approximations

In order to quantify how well the current AACGM coefficients reproduce AACGM coordinates, the results obtained from using the AACGM coefficients on a 1° latitude by 5° longitude geographic grid are compared to the results obtained from determining the AACGM coordinates by numerical field-line tracing on the same grid. A Runge-Kutta-Fehlberg adaptive step-size, ordinary differential equation (ODE) solver was developed in order to accurately follow magnetic field lines in the IGRF model. Tests using a 1 km fixed step-size Runge-Kutta 4th order ODE solver show that limiting the maximum step-size to $50 r^3$ km (where r is the distance from the origin in units of Earth radii R_E) keeps the overall difference observed using the adaptive step-size solver to below 1 km for the entire grid. For this study the upper limit on the accuracy of the numerical field-line tracing is therefore considered to be ~ 1 km.

Spherical harmonic functions are evaluated using the standard AACGM software that has been available from the Johns Hopkins University Applied Physics Laboratory since the coordinate system was developed by *Baker and Wing* [1989]. This software includes the AACGM coefficients for the 5-year epochs from 1975 to 2010. Differences between the AACGM coordinates obtained from the coefficients and those obtained from the numerical field-line tracing are measured in great-circle distance on the surface of the Earth. The observed differences are considered to be errors associated with using the AACGM coefficients to obtain the exact (to within 1 km) AACGM coordinates. Note that in order to determine the great-circle distance, it is necessary to compute the inverse transformation from AACGM to geographic coordinates. This transformation is computed using the adaptive step-size ODE solver, as described in section 6, in order to minimize any additional numerical error.

Figure 2 shows several maps of the error associated with the AACGM coefficients for an altitude of 0 km (i.e., the surface of the Earth) for the representative years 1995, 2000, 2005, and 2010. The color scale indicates the magnitude of the error from 0–100 km at each grid location. White indicates locations where the error is larger than 100 km and grey indicates that the AACGM coordinates are not defined for this location, i.e., the forbidden region. Continent outlines are shown for reference and colored stars indicate the locations of SuperDARN radar sites in both hemispheres.

It can be seen from the maps in Figure 2 that different techniques were likely used to obtain the AACGM coefficients for these particular epochs. Figure 2a and 2b show similar features suggesting the same technique was used for epochs 1995 and 2000, however, the overall error appears to be larger in 2000. Figure 2c shows much lower errors overall in the polar regions, apparently at the expense of a region of very large error just poleward of the undefined region (grey) at longitudes from -60° to 60° . Finally, for the current epoch, Figure 2d shows numerous regions of larger (>50 km) error with lower error near $\pm 50^\circ$ and $\pm 90^\circ$ latitude. In all cases errors exceeding 10 km are present over a significant portion of the globe.

The source of the unexpectedly large errors, particularly away from the equator, is a consequence of the difficulty in fitting a continuous function through regions where the solution does not exist. In particular, the large area that extends from approximately -10° to 30° latitude and -60° to 60° longitude is a region where the AACGM coordinates are undefined. In this region, the higher-order terms of the magnetic field model contribute significantly to the non-dipolar nature of the field. The magnetic dip equator in this region is significantly offset from the dipole equator, and magnetic field lines originating in one hemisphere intersect the magnetic equator below the surface of the Earth (see Figure 1.)

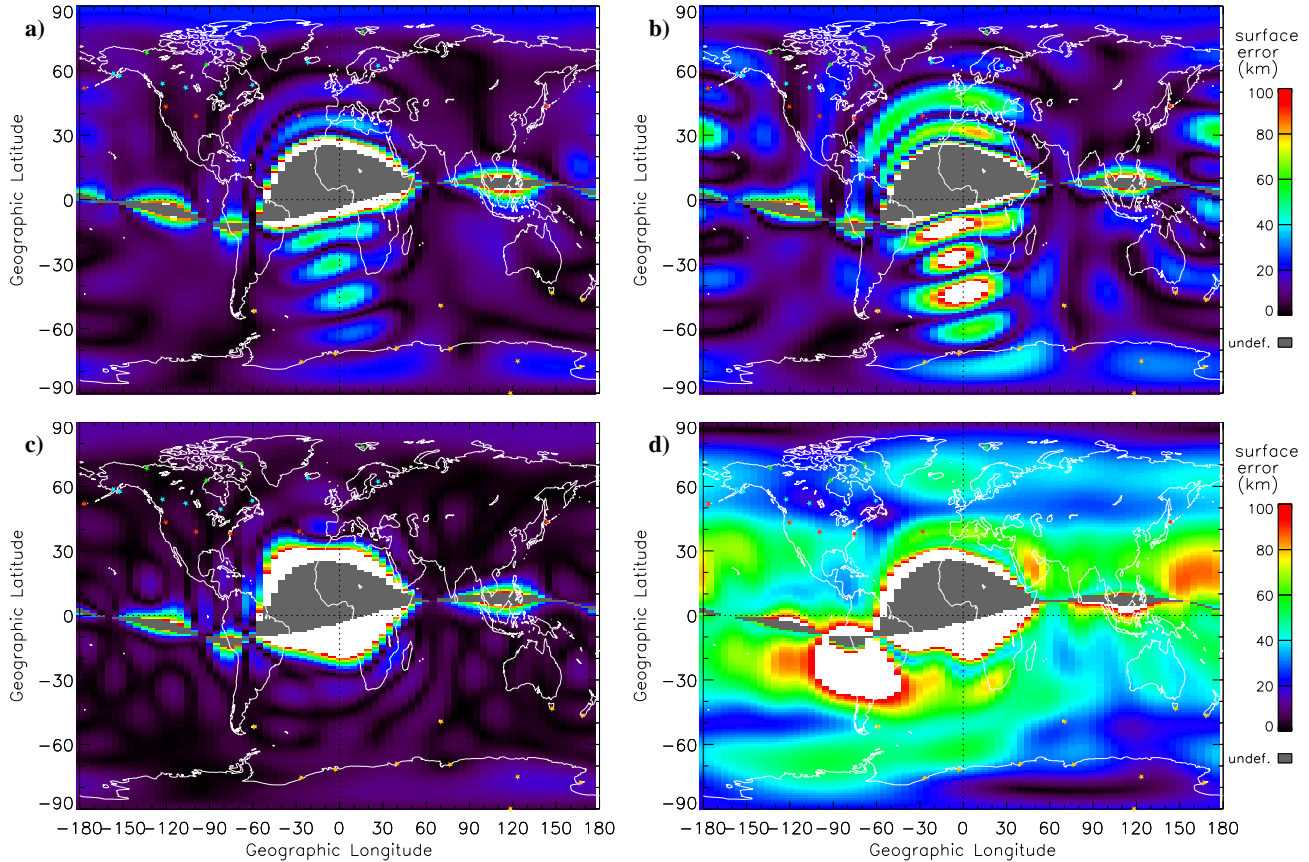


Figure 2. Error associated with using AACGM coefficients to obtain AACGM coordinates on geographic grid for 0 km altitude for the years (a) 1995, (b) 2000, (c) 2005 and (d) 2010. Color indicates error in great-circle distance at the surface of the Earth. Regions shown in grey are areas where AACGM coordinates are undefined. Colored stars indicate locations of SuperDARN radars.

Developments related to the technique used to determine AACGM coefficients have primarily focused on a better representation in this region, which is related to the SAA. Several different approaches have been used to cope with the difficulties associated with the forbidden region. While *Baker and Wing* [1989] follow the approach used by *Gustafsson* [1984] and simply exclude a band of data within 24° of the equator, other authors have taken the approach of adding additional data points to this region before deriving the AACGM coefficients. *Gustafsson et al.* [1992] uses linear interpolation between the last defined CGM points and the magnetic dip equator, defined in two different ways, to specify the CGM latitude in the so-called forbidden region. Tabulated data obtained using both methods of describing the magnetic dip equator are included in appendices of their paper.

More recent studies have augmented the tabulated AACGM data using an alternative definition in forbidden regions before deriving the AACGM coefficients. *Bhavnani and Hein* [1994] and *Hein and Bhavnani* [1996] use a spline fit through a band of $\sim 15^\circ$ around the magnetic equator to fill in missing grid points at each longitude. An additional requirement that the spline fit latitude obeys the dip equator is imposed. Inspection of Figure 1 of *Bhavnani and Hein* [1994] suggests that data points are either compressed in latitude in this region or a finer sampling is used. *Heres and Bonito* [2007] use a technique to perform additional smoothing of interpolated data in the forbidden region by distributing points more uniformly according to spatial derivatives of the grid.

In all cases, additional data have been added to the tabulated AACGM data in the forbidden regions, i.e., the regions where AACGM is not defined. It is because of the emphasis

on defining a solution in this region that the accuracy of the AACGM coefficients has degraded at higher latitudes.

Figure 3 shows the Cartesian components of the AACGM coordinates obtained from both the field-line tracing and the AACGM coefficients over the full range of geographic latitude. This example is taken along the prime meridian, i.e., 0° longitude, which corresponds to the vertical dotted line in each panel of Figure 2. Coordinates obtained from field-line tracing are shown in the bottom panel as red crosses, with solid red lines added for emphasis. Coordinates obtained from the AACGM coefficients are overlotted using blue circles.

The forbidden region at this longitude extends over the latitude range -5° to 25° and is indicated by the solid grey area. The difficulty in approximating AACGM coordinates in this region can most clearly be seen in the z component where the data are discontinuous across the forbidden region. Although the interpolated data used to augment the AACGM data are not known, and therefore not shown, coordinates obtained from the AACGM coefficients show that they strongly influence the solution in this region. Close inspection of these curves reveals that the solution oscillates about the field-line traced data throughout the full latitude range. The upper panel of Figure 3 shows the difference between the two normalized coordinates. While the magnitude of this error decreases with distance from the forbidden region, the oscillation is apparent. Note that the more weighting or emphasis that is placed on data in the forbidden region, the larger the resulting oscillations will be.

4. AACGM Coefficients

In this study, a different approach is used to derive a new set of AACGM coefficients. This approach can be summarized by the principle that a set of coefficients be obtained which most accurately represent the AACGM coordinates, ideally over the largest area possible, but with particular interest in the middle to polar latitude region and altitudes up to 2000 km.

The main differences in this technique are that in order to stay true to the AACGM coordinates, the AACGM data are in no way augmented, i.e., no additional points are added to the forbidden region. The solution is simply undefined in this region. As discussed in section 3, the addition of data to the forbidden region causes undue error at higher latitudes. This problem is avoided by simply using AACGM data on a regular geographic grid, where it is defined.

Secondly, a normalization scheme that is different from previous studies is used. Equation 2 does not guarantee that the resulting points are confined to the surface of a sphere and points must therefore be normalized to the unit sphere. Instead, x_m and y_m from equation 2 are used to determine z_m by requiring that the position be located on the surface of the Earth, i.e., $z_m = \sqrt{1 - x_m^2 - y_m^2}$, where the Cartesian coordinates have been normalized by the Earth radius. Note that the coefficients A_{lm}^z are still used but only to determine the sign of z_m in order to locate each point in the correct hemisphere.

This simple modification leads to significantly improved accuracy of the resulting AACGM coefficients over the entire range of latitudes. It is worth acknowledging that this strategy leads to a solution that is not always defined continuously along a given meridian (i.e., z_m can be imaginary where $x_m^2 + y_m^2 > 1$ in the forbidden region), but argue that the benefits of a much better fit outweigh this disadvantage in many situations where conversions from geographic to AACGM coordinates are used.

Figure 4 shows the result of the new AACGM coefficients along the prime meridian, as in Figure 3, i.e., 0 km altitude and for the year 2000. In this case AACGM coordinates obtained from using the new AACGM coefficients are shown

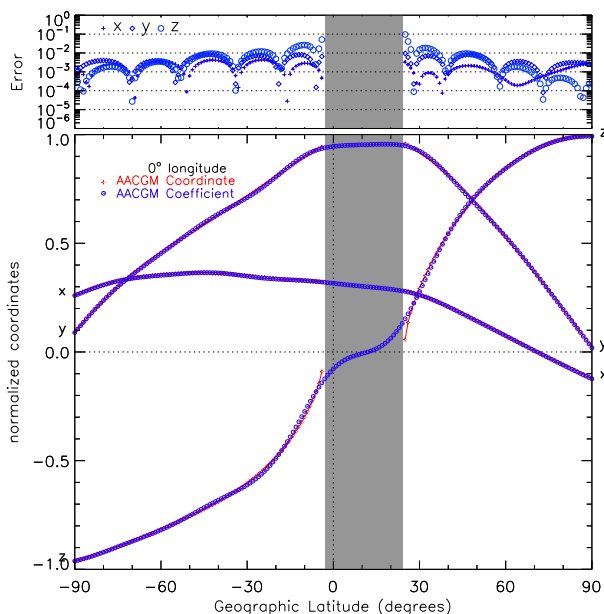


Figure 3. Cartesian coordinates, obtained from field-line tracing (red) and AACGM coefficients (blue) along the prime meridian in Figure 2b. Solid grey indicates the forbidden region. Errors are shown on a logarithmic scale for each coordinate in the top panel.

in green. Comparing to Figure 3 the agreement with the AACGM data is significantly improved over the entire latitude range. Error for each coordinate is shown in the top panel with values from Figure 3 included for direct comparison. While variation is observed in the use of both sets of coefficients, the error obtained from the new coefficients is 1–2 orders of magnitude lower than that resulting from use of the current coefficients. Similar results are observed for all longitudes.

New sets of AACGM coefficients have been determined using this new technique. For each 5-year epoch a grid of 1° latitude and 5° longitude is used. A one-to-one mapping

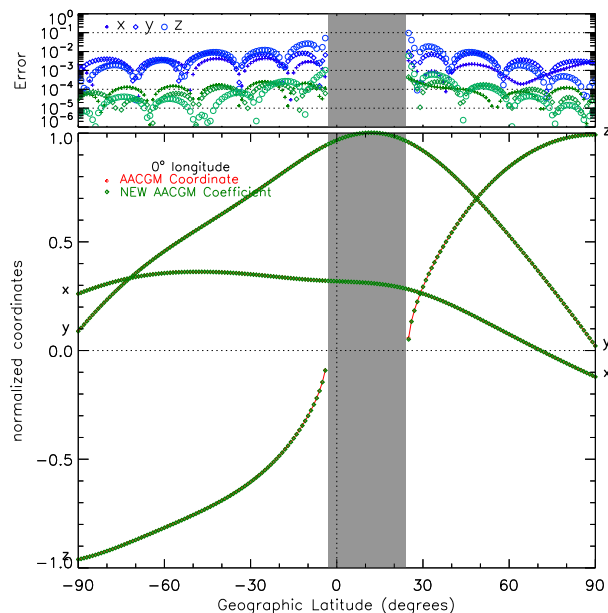


Figure 4. Cartesian coordinates obtained from field-line tracing (red) and new AACGM coefficients (green) along the prime meridian in Figure 2b. Solid grey indicates the forbidden region. Errors are shown on a logarithmic scale for each coordinate in the top panel.

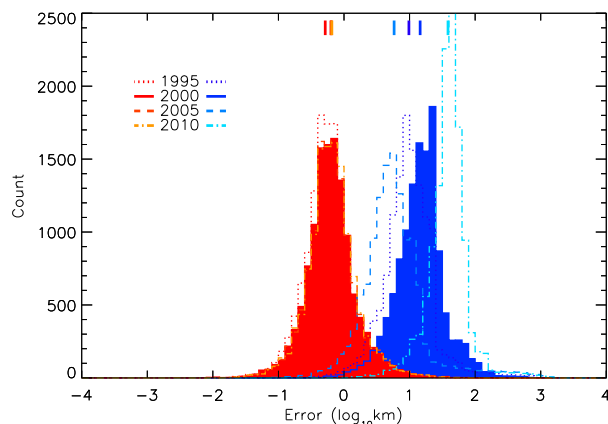


Figure 5. Distribution of errors in AACGM coordinates using the existing and new AACGM coefficients from Figures 2 and 6. Errors are binned on a logarithmic scale. Blue and red colors represent the existing and new coefficients, respectively. Solid histograms represent data for the year 2000. Average errors are indicated at the top of the figure by small vertical lines.

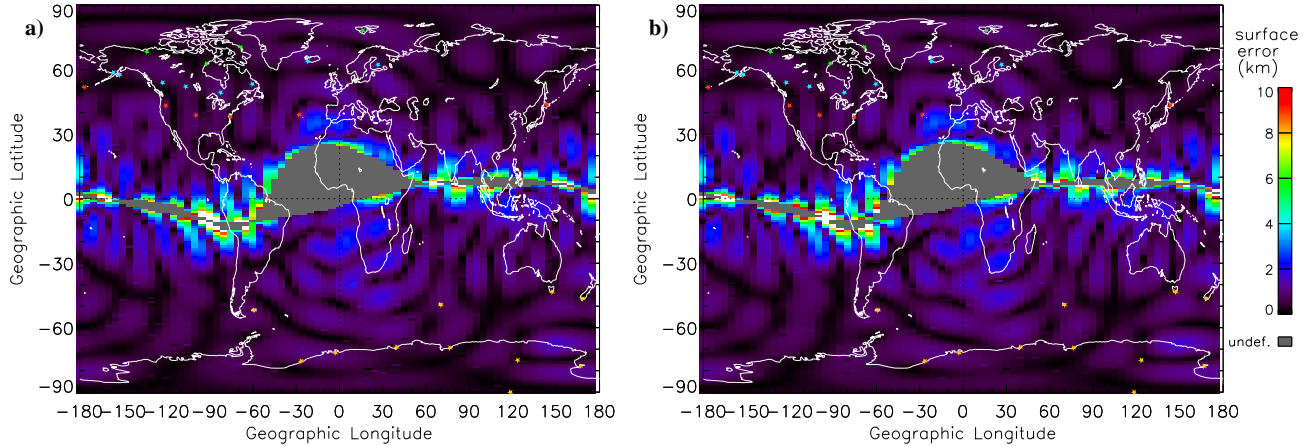


Figure 6. Error maps identical to Figure 2b and 2d but using the new AACGM coefficients and the color scale range is 0–10 km.

from geographic to AACGM coordinates is obtained using the adaptive step-size ODE solver for each geographic grid point. These data are then used to determine the AACGM coefficients from equation 2. A standard singular value decomposition scheme is used to obtain the coefficients $\{A_{lm}^x, A_{lm}^y, A_{lm}^z\}$ for each 5-year epoch.

As was the case for the existing coefficients, the new coefficients are used to determine the corresponding AACGM coordinates on the same geographic grid. Error maps at 0 km altitude for the years 2000 and 2010 are shown in Figure 6 using the same format as that in Figure 2, with the exception that the color scale is an order of magnitude smaller (0–10 km) in order to show where errors exist. Note that maps for the other years are nearly identical to those shown.

Comparison of the corresponding maps in Figures 2 and 6 confirms the significant improvement in the accuracy realized over the entire globe when using the new coefficients to determine AACGM coordinates. With the exception of a region extending a few degrees from the forbidden regions, the observed errors are limited to ~ 1 km.

Histograms of the distribution of errors on a logarithmic scale are plotted in Figure 5 for the four years shown in Figures 2 and 6 (1995 and 2005 data are included). Blue and red histograms represent the errors associated with using the existing and new AACGM coefficients, respectively. Average errors are indicated at the top of the figure with vertical lines matching the color of the corresponding histogram below. To emphasize the difference between the two techniques a solid histogram is shown for each set of coefficients for the year 2000.

Average errors using the existing coefficients are in the range of a few to tens of kilometers while the corresponding average errors using the new coefficients are < 1 km. Large errors exceeding 100 km can result from using the existing AACGM coefficients and extend to middle latitudes; e.g. Figure 2b. Using the new coefficients, only a small portion of the data have errors that exceed 1 km. Inspection of Figure 6 reveals that these larger errors are limited to a small region poleward of the forbidden region.

Overall, the new AACGM coefficients show a significant improvement over the existing coefficients. Errors are 1–2 orders of magnitude lower and limited to less than ~ 1 km over the region of interest. A potential drawback associated with the new coefficients is that they are undefined in the so-called forbidden region and therefore do not provide a continuous solution throughout this region. It is worth repeating that the intent of this work is to provide a set of approximating functions (AACGM coefficients) that represent AACGM coordinates to a high degree of accuracy.

5. Altitude Dependence

Attention is now turned to the altitude dependence of the AACGM coordinates. As described in section 2 the procedure for determining AACGM coefficients at the surface of the Earth (0 km altitude) is repeated at multiple reference altitudes in order to obtain a set of coefficients that are then either interpolated or fit to a polynomial function in altitude.

Figure 7 shows the Cartesian AACGM coordinates obtained from both sets of coefficients (old and new) at an altitude of 2000 km for the prime meridian and in the same format as Figures 3 and 4. Here, both sets of coordinates are combined with blue and green indicating the old and new coefficients, respectively. AACGM coordinates obtained from

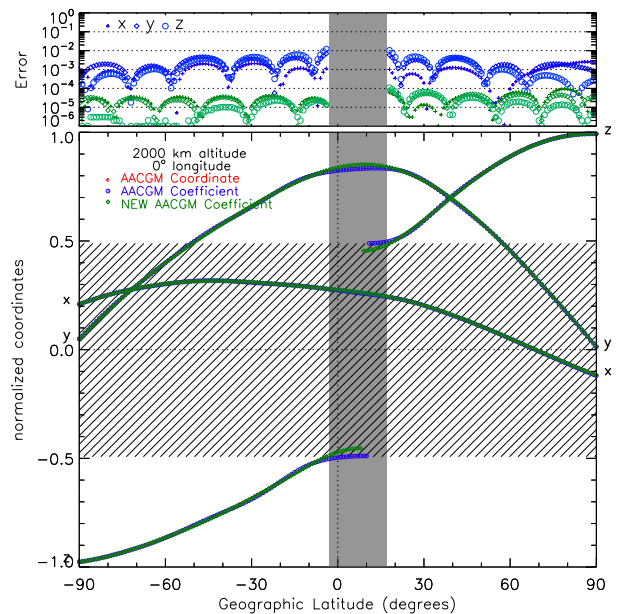


Figure 7. Cartesian coordinates obtained from field-line tracing (red) and old (blue) and new (green) AACGM coefficients along the prime meridian for the year 2000 and for 2000 km altitude. The format is similar to Figures 3 and 4 with a hatched area added to indicate the region where AACGM latitudes are not accessible at this altitude.

field-line tracing are again shown in red, but are admittedly difficult to see at most latitudes due to the accuracy of the values obtained from both sets of coefficients. Errors associated with these values are shown in the upper panel on a logarithmic scale.

One immediate difference observed at this altitude is the large discontinuity in the z coordinate near the geographic equator and indicated by hatching in the figure. This region represents the range of AACGM latitudes which are not accessible for the given altitude; 2000 km in this case. In this region the magnetic equator is located below the altitude where magnetic field-line tracing begins and these latitudes are, therefore, not attainable. This region is determined by the latitude of the dipole field line with L -shell value equal to the geocentric distance above the surface of the Earth, $(R_E + h)/R_E$. Latitudes below λ_0 , given by

$$R_E = (R_E + h) \cos^2 \lambda_0 \quad (4)$$

are not accessible for the altitude h , and a discontinuity in the z coordinate exists over this range. For the altitude $h = 2000$ km, shown in Figure 7, $\lambda_0 = 29.3^\circ$.

In order to minimize the undesirable effects associated with approximations near such a discontinuity, *Bhavnani and Hein* [1994]; *Hein and Bhavnani* [1996]; *Heres and Bonito* [2007] use a simple mapping given by

$$\cos \lambda_{\text{dipole}} = \left(\frac{R_E + h}{R_E} \right)^{\frac{1}{2}} \cos \lambda_m, \quad (5)$$

where the magnetic latitude λ_m is mapped to what the authors refer to as an “at-altitude dipole coordinate system” given by λ_{dipole} . In this “at-altitude coordinate system”, λ_0 maps to the equator, effectively eliminating the discontinuity. In these studies, AACGM coefficients are derived using “at-altitude coordinates” and the inverse mapping is used to determine AACGM coordinates from the “at-altitude coordinates”.

Because the z coordinate is computed from the x and y coordinates this additional mapping is not required and “at-altitude coordinates” are, therefore, not used in the calculations. Inspection of Figure 7 confirms that the functional representation all three Cartesian coordinates is sufficiently accurate at non-zero altitudes when using the new coefficients. The upper panel shows that errors resulting from the new coefficients are again 1–2 orders of magnitude lower than those resulting from the old coefficients. A similar reduction of error is observed at all altitudes from 0–2000 km.

As with the 0 km altitude comparisons, the same analysis is performed at 2000 km by comparing AACGM coordinates over the same geographic grid. Figure 8a shows the resulting error when using the existing AACGM coefficients for the year 2000. The color scale is the same as that used in Figure 2. Comparing the two altitudes, it can be seen that overall errors have decreased at 2000 km altitude, where the field becomes more dipolar and the solution becomes easier to approximate. Errors exceeding 50 km, however, are still observed in some regions.

For comparison, Figure 8b shows the resulting errors when using the new AACGM coefficients for the year 2000 at 2000 km altitude. The color scale is the same as that used in Figure 6 and an order of magnitude lower than in Figure 8a. In this case the errors are again lower than at 0 km altitude and significantly lower than those resulting from the existing AACGM coefficients.

In order for AACGM coordinates to be determined from AACGM coefficients at a continuous range of altitudes, some form of altitude-dependence is required of the coefficients. As described briefly in sections 2 and 4, the procedure to determine a set of AACGM coefficients for a particular altitude

is repeated for several reference altitudes. The coefficients needed for a general altitude h are then determined by one of several techniques. *Baker and Wing* [1989] suggest that simple linear interpolation of the coefficients at the reference altitudes can be used. Subsequent studies have used functional forms of the coefficients to represent their altitude dependence. *Bhavnani and Hein* [1994] use a quadratic polynomial to interpolate the coefficients at reference altitudes, whereas *Hein and Bhavnani* [1996]; *Heres and Bonito* [2007] fit a quartic polynomial to the reference altitude coefficients with weighting that limits the amount of variation in the fit at 0 km altitude and improves the fit in the 0–1200 km region. However, the exact weighting used by *Hein and Bhavnani* [1996]; *Heres and Bonito* [2007] is unknown, as well as the locations of the 24 reference altitudes used by *Hein and Bhavnani* [1996].

In addition to the use of increasingly higher-order polynomials by authors, the altitude range over which the AACGM coefficients are valid has increased from 600 km [*Baker and Wing*, 1989] to 2000 km [*Bhavnani and Hein*, 1994] to its current value of 7200 km [*Hein and Bhavnani*, 1996; *Heres and Bonito*, 2007]. As several authors state, the coefficients typically vary quite smoothly in altitude, which is used as justification for performing a low-order polynomial approximation. Note, however, that over the 7200 km altitude range many of the coefficients vary enough that a quartic fit is insufficiently accurate over the entire range, particularly at altitudes below ~ 1000 km. It is for this reason that *Hein and Bhavnani* [1996]; *Heres and Bonito* [2007] use a weighted fit to improve the accuracy in this region. Without knowledge of the weighting used it is not possible to verify the accuracy of their techniques.

After studying the altitude behavior of the coefficients, a similar approach is taken here, however, the altitude range is limited to 2000 km. The limitation is deemed necessary in order to improve accuracy of the coefficients in the altitude range that includes the upper limit of LEO. Above 2000 km, AACGM coordinates are still defined, but they should be obtained using field-line tracing in order to ensure accuracy.

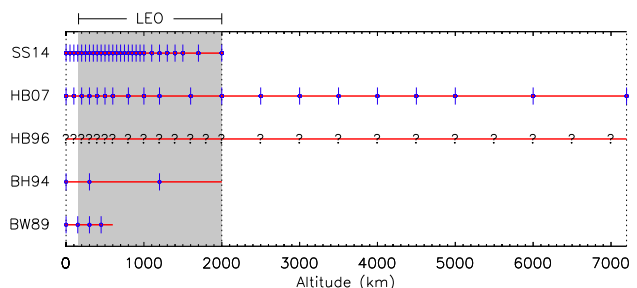


Figure 8. Altitude range (red lines) and reference altitudes (blue vertical line-segments) used to determine the altitude dependence of AACGM coefficient sets for the different studies. Details and abbreviations for the studies are listed in Table 1.

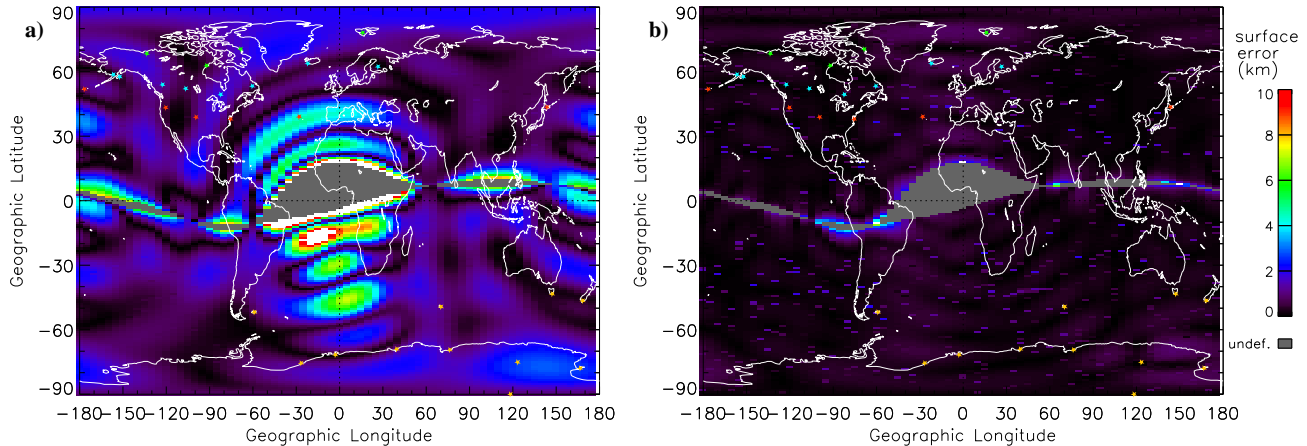


Figure 9. Error associated with using AACGM coefficients to obtain AACGM coordinates for 2000 km altitude. The format is the same as for Figures 2b and 6b. The color scales are 0–100 km and 0–10 km for the (a) old and (b) new AACGM coefficients.

Table 1. Altitude Dependence of AACGM Coefficients

Study	Reference Altitudes (km)	Approximation Scheme	Altitude Range (km)
BW89 ^a	0, 150, 300, 450	interpolation	0–600
BH94 ^b	0, 300, 1200	quadratic	0–2000
HB96 ^c	24 unspecified values between 0–7200 km	weighted quartic fit	0–7200
HB07 ^d	0, 100, 200, 300, 400, 500, 600, 800, 1000, 1200, 1600, 2000, 2500, 3000, 3500, 4000, 4500, 5000, 6000, 7200	weighted quartic fit	0–7200
SS14 ^e	0, 50, 100, 150, 200, 250, 300, 350, 400, 450, 500, 550, 600, 650, 700, 750, 800, 850, 900, 950, 1000, 1100, 1200, 1300, 1400, 1500, 1700, 2000	modified quartic fit	0–2000

^a Baker and Wing [1989]

^b Bhavnani and Hein [1994]

^c Hein and Bhavnani [1996]

^d Heres and Bonito [2007]

^e this study

Following Hein and Bhavnani [1996]; Heres and Bonito [2007], a quartic fit is used to approximate the altitude dependence of the coefficients for this study. However, the reference altitudes used here differ from previous studies and are specified in Table 1 and shown in Figure 9. The reference altitudes selected for this study are spaced such that they better describe the altitude behavior of the coefficients at lower altitudes, where more rapid changes are most often observed. For comparison, the altitude dependence of each study is also summarized in Table 1 and reference altitudes are indicated by blue vertical line-segments in Figure 9. Note that the locations of the unspecified reference altitudes for the Hein and Bhavnani [1996] study are indicated by question marks in Figure 9.

One additional point that is important to mention is that this author feels it important that the AACGM coordinates derived from the coefficients at 0 km altitude should be an accurate representation of CGM coordinates [Gustafsson, 1984; Gustafsson et al., 1992]. For this reason a requirement is made that the quartic fits retain the value of the coefficients at 0 km altitude and fit the remaining coeffi-

cients of the quartic to the AACGM coefficients at the set of reference altitudes given in Table 1.

Figure 11 shows the altitude dependence of two representative coefficients ($A_{2,0}^x$ and $A_{5,-5}^y$) over the 0–2000 km altitude range. The value of these particular coefficients at each reference altitude is shown by a black circle. The solid orange line in each panel represents the quartic fit to the reference altitudes. It is the coefficients of the $3(N+1)^2$ quartic fits that constitute the set of AACGM coefficients, which are then used to determine AACGM coordinates in the same manner as Hein and Bhavnani [1996]; Heres and Bonito [2007]. These coefficients provide a means for determining AACGM coordinates over a continuous range of altitudes h from 0–2000 km.

As stated by previous authors, the coefficients vary quite smoothly and the quartic fits are quite accurate, as evidenced by the near collocation of the black circles and the orange lines. Differences between the quartic fit and the values at reference altitudes are represented by orange crosses on a logarithmic scale in the bottom panels of Figure 11.

Two additional quartic fits are shown in Figure 11 as dotted lines. These fits are performed using additional reference altitudes that extend to 7200 km (not shown.) One of the additional fits includes the 0 km reference altitude and the other requires that the fitted polynomial pass through the value at 0 km. Errors for both additional fits are represented in the lower panels by blue and purple crosses, respectively.

Justification for limiting the altitude range to 2000 km is evidenced by the relatively poor fit of the polynomials that use the full 7200 km altitude range, particularly over the altitude range shown. The lack of agreement is particularly evident in Figure 9b, where the additional polynomial fits poorly represent the observed values. Note, however, that the absolute errors are equally large for the $A_{2,0}^x$, despite the apparent agreement.

Extending the altitude range to 7200 km has clearly reduced the accuracy of the polynomial fits. While Hein and Bhavnani [1996]; Heres and Bonito [2007] use unspecified weights to improve the accuracy of the fits at lower altitudes, it is beyond the scope of this work to fully assess the impact of various weighting schemes on the accuracy of the fits over the entire altitude range. Instead, in keeping with the aim of this work, the altitude range has been limited to 2000 km in order to maintain accuracy of the functional approximations used to describe the altitude dependence of the coefficients over this range. The improvement is clearly demonstrated by the overall lower error observed in the polynomials fits to the limited altitude range.

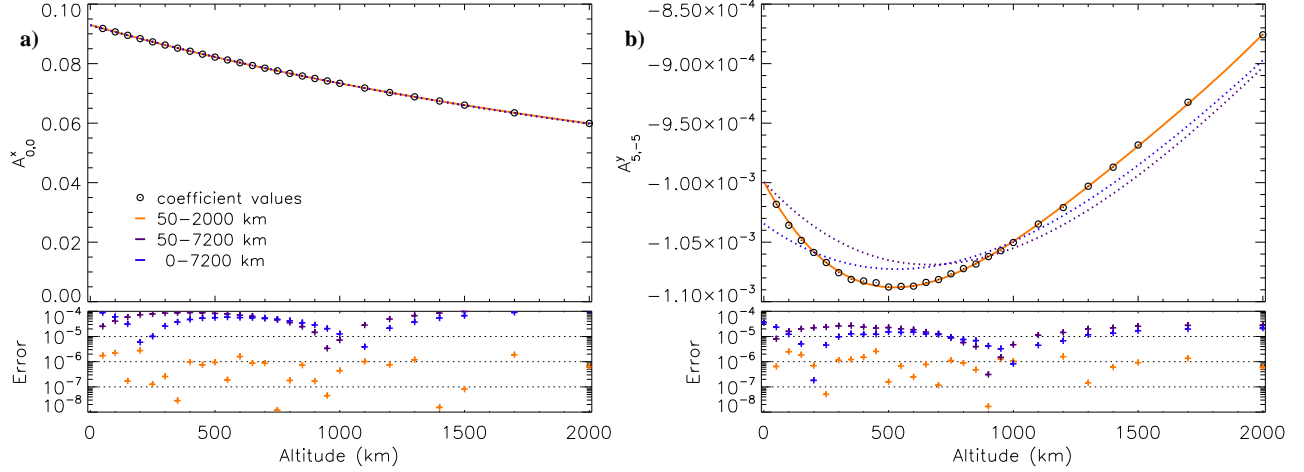


Figure 10. Altitude dependence of two AACGM coefficients: (a) $A_{2,0}$ and (b) $A_{5,-5}$ for each Cartesian component. Values obtained at reference altitudes are indicated by black circles. Orange solid lines represent the quartic fits to reference altitudes over the range shown. Dotted lines represent quartic fits using reference altitudes that extend to 7200 km. One fit includes the value at 0 km altitude (blue) and the other passes through this value (purple). Errors associated with the fits are shown in the lower panels as crosses in the corresponding color of the fit.

While error maps shown in Figures 6 and 8b demonstrate that AACGM coefficients with relatively low errors can be obtained at discrete altitudes, it is the quartic functions that approximate the altitude dependence of the coefficients that are used in practice. In order to demonstrate sufficient accuracy of the altitude-dependent coefficients, further investigation is performed on the following representative altitudes: 0, 333, 600, 1850 km. Two of these altitudes are part of the set of reference altitudes, the other two are at the lower and upper ends of the altitude range.

For each of these representative altitudes field-line tracing is performed to determine the AACGM coordinates for each point on the geographic grid. AACGM coordinates are also determined using the old and new AACGM coefficients, and errors are then computed in the same manner as described in section 3. Instead of showing error maps, as before, histograms of the distribution of observed errors are computed

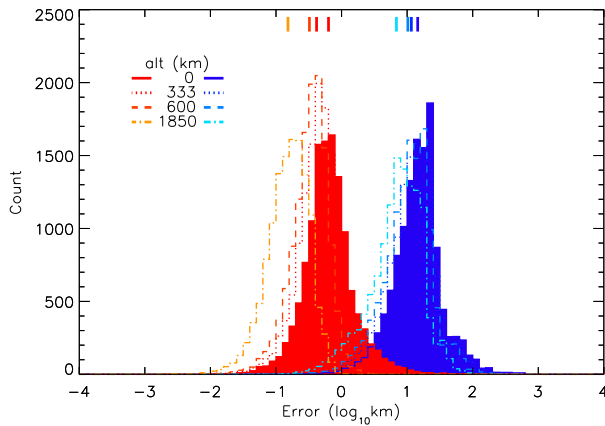


Figure 11. Distribution of errors in AACGM coordinates using the existing and new AACGM coefficients for altitudes 0, 333, 600, 1850 km. Errors are binned on a logarithmic scale. Blue and red colors represent the existing and new coefficients, respectively. Solid histograms represent data for 0 km altitude and are identical to the corresponding histograms in Figure 5. Average errors are indicated at the top of the figure by small vertical lines.

and binned on a logarithmic scale in the same manner as shown in Figure 5. The year 2000 has been selected in order to make comparisons to other figures.

Figure 10 shows error histograms for each of the four representative altitudes. Red and blue colors indicate errors associated with the new and old coefficients, respectively. The solid histograms are chosen to emphasize errors at 0 km altitude. Because the AACGM coefficients at 0 km altitude have been included when performing the quartic coefficient fits, the solid histograms are identical to those in Figure 5. The other histograms correspond to errors associated with using the altitude-dependent coefficients and are not neces-

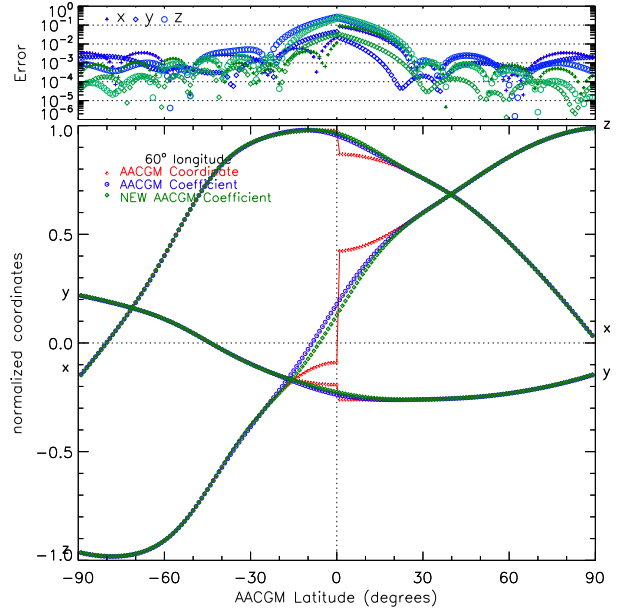


Figure 12. Geographic Cartesian coordinates obtained from field-line tracing (red) and old (blue) and new (green) inverse AACGM coefficients along the 60° AACGM meridian at the surface of the Earth. The format is similar to Figure 7.

sarily the same as those obtained from using the AACGM coefficients at these altitudes. Comparison of AACGM coordinates obtained from both the altitude-dependent coefficients and the actual AACGM coefficients at these same altitudes, reveals that differences are less than 1 km in all cases when using the new coefficients. It is not possible to make a similar statement about the old coefficients because the AACGM coefficients at the reference altitudes are not known.

To summarize the altitude dependence of AACGM coefficients, the altitude range over which the coefficients are valid has been limited to 2000 km. AACGM coefficients are determined at 28 reference altitudes (shown in Table 1 and Figure 9) and quartic polynomial fits are performed on each coefficient. The accuracy of these altitude-dependent coefficients is characterized by errors that (1) are typically below 1 km (with the exception of latitudes within a few degrees of the forbidden region), (2) are 1–2 orders of magnitude smaller than those associated with the existing coefficients and (3) decrease in magnitude with altitude (as shown in Figure 10).

6. Inverse Transformation

In order to obtain geographic coordinates from AACGM coordinates an inverse transformation is required. Following the definition of AACGM coordinates in section 2, geographic coordinates are determined by following the magnetic field line from the starting point on the magnetic equator to the desired altitude h . The final position gives the desired geographic coordinates. The starting point is given by the coordinates of the dipole field line that connects the surface of the Earth and the magnetic equator.

Previous studies have used various techniques to determine a set of mapped data at different altitudes from which to determine the corresponding inverse AACGM coefficients. These inverse coefficients are derived in the same manner as those of the forward transformation (geographic to AACGM). In this case the geographic Cartesian coordinates (x_g, y_g, z_g) are written as an expansion of spherical harmonic functions in the magnetic co-latitude and longitude

variables (θ_m, ϕ_m) , following equation 2. The set of coefficients for the inverse transformation $\{B_{lm}^x, B_{lm}^y, B_{lm}^z\}$ are again determined by fitting a quartic function to the coefficients determined at the same reference altitudes. The set of forward (A) and inverse (B) coefficients comprise a complete set of AACGM coefficients that are used to convert to and from AACGM coordinates.

Investigation of the inverse transformation reveals a few difficulties. The first challenge is related to the SAA and the associated discontinuity observed at the magnetic equator (see Figures 3 and 4). Figure 12 shows the normalized geographic coordinates (x_g, y_g, z_g) as a function of AACGM latitude (λ_m) for the 60° AACGM meridian, in the same format as Figure 7. At this meridian the discontinuity at the magnetic equator is pronounced in the geographic coordinate data (shown by red lines and obtained from tracing magnetic field lines following the inverse process.)

In the forward transformation the discontinuity was seen only in the z_m coordinate, i.e., the magnetic latitude. The solution to use the values of the other two coordinates and the condition that the three components be confined to the surface of the Earth, worked well for that case. For the inverse transformation, however, the discontinuity appears in each component (x_g, y_g, z_g) because of their dependence on θ_m . For the inverse case it is not possible to avoid fitting an expansion of spherical harmonic functions to a discontinuous set of data. In order to minimize the resulting oscillations, a limited range of latitudes near the discontinuity are excluded from the data used in the fittings. Because it leads to a slightly overall better fit, the same dataset used for the forward transformation is used for the inverse transformation, i.e., a regular geographic grid mapped to an irregular AACGM grid.

Experimentation reveals that excluding a range of latitudes that extends poleward of the forbidden region (in geographic coordinates) reduces the errors observed in the fittings over the full range of latitudes. Beyond some range, however, the errors begin to increase. It is found that excluding data that extends 10° poleward of the forbidden region for each longitude leads to a reasonable compromise between reducing the average and maximum errors observed. This same data exclusion is used for all reference altitudes.

Figure 12 shows the resulting fits for the 60° AACGM meridian in addition to the errors associated with the fits. Near the discontinuity errors are seen to be quite large, which is expected. However, the resulting errors are somewhat reduced from the existing AACGM inverse coefficients for magnetic latitudes poleward of the equator.

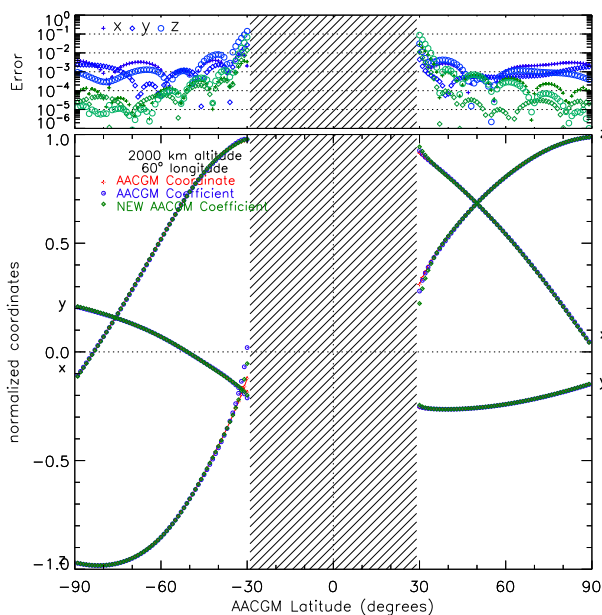


Figure 13. Geographic Cartesian coordinates for the 60° AACGM meridian in the same format as Figure 12 but for 2000 km altitude.

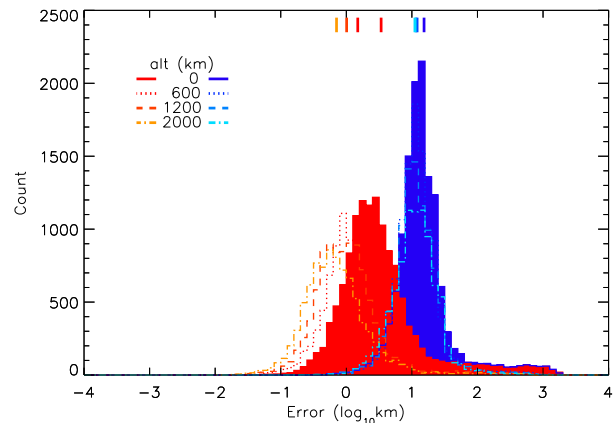


Figure 14. Distribution of errors in determining geographic coordinates using the existing and new AACGM inverse coefficients for altitudes 0, 600, 1200, 2000 km. Errors are binned on a logarithmic scale and the format is the same as Figure 10.

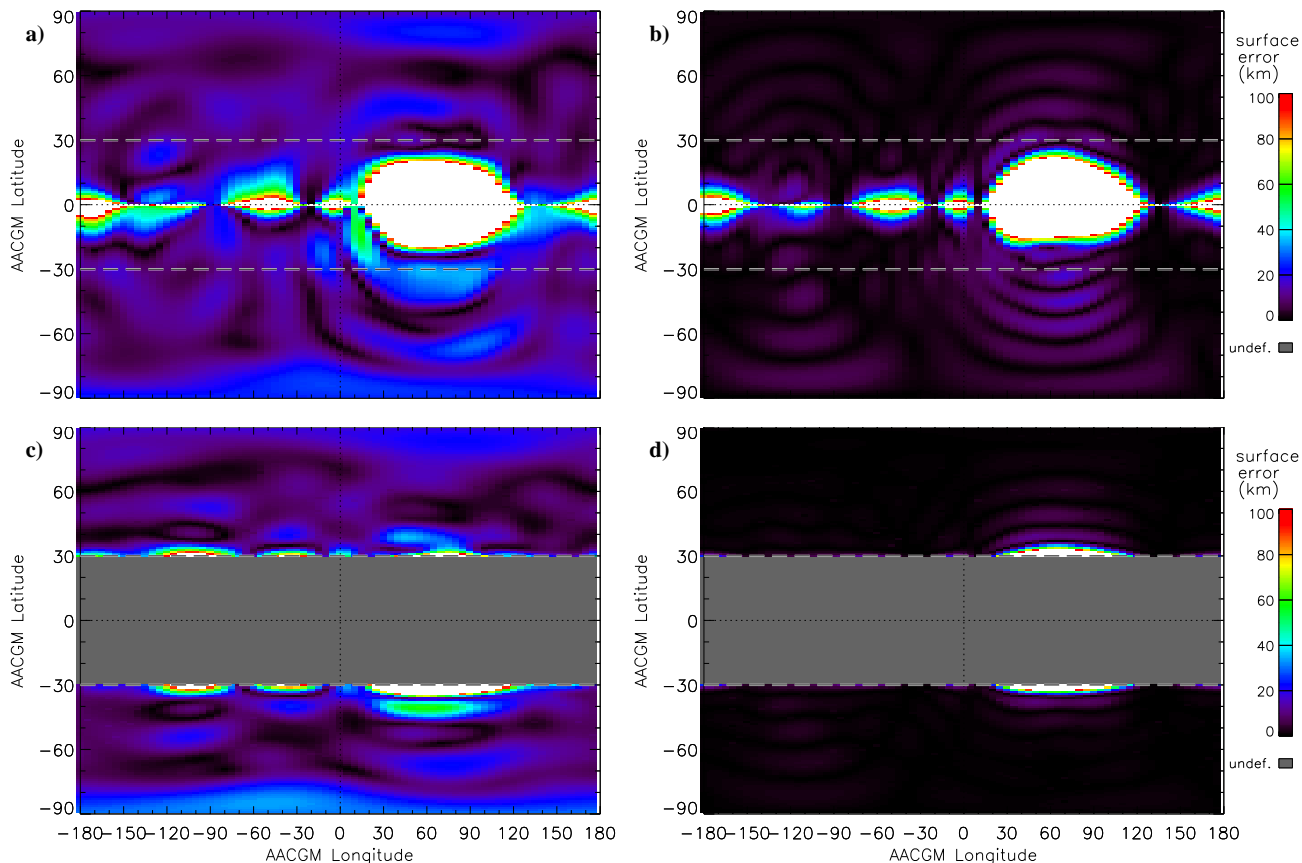


Figure 15. Error associated with using AACGM inverse coefficients to obtain geographic coordinates for (a–b) 0 km altitude and (c–d) 2000 km altitude. The color scale is the same for the (a,c) old and (b,d) new AACGM coefficients.

An additional complication to the inverse transformation is the fact that AACGM coordinates are not defined at magnetic latitudes below λ_0 , given by equation 4, for non-zero altitudes h . Figure 13 shows the Geographic Cartesian coordinates for the same 60° AACGM meridian as Figure 12 but for an altitude of 2000 km. At this altitude $\lambda_0 = 29.3^\circ$, as shown by the hatched region in Figure 13. In the case of the inverse transformation there is an added benefit to using the “at-altitude dipole coordinate system” given by equation 5, which is not the case for the forward transformation. The reduction in error when using the new inverse coefficients can be seen in the top panel of Figure 13 along with the errors associated with the existing inverse coefficients.

Figure 15 shows error maps in the same format as Figure 8 but for the inverse transformations at altitudes of 0 km and 2000 km. The errors again are the difference in the great circle distance between the position obtained from the AACGM inverse coefficients and the field-line tracing, i.e. the actual coordinates (to within the ~ 1 km accuracy discussed in section 3.)

The color scales are the same for each panel and show a modest improvement in the error associated with the new AACGM inverse coefficients. The reduction in error is not as large as was the case in the forward transformation and relatively large errors are seen to occur below $\sim 30^\circ$, particularly near the SAA region; 30° – 120° AACGM longitude. Above $\sim 30^\circ$ (marked with dashed lines) errors in the tens of kilometers are visible. While these errors are larger than those observed in the forward case, they are a definite improvement over the existing AACGM inverse coefficients, where errors are more than twice as large.

Figure 14 shows the distribution of errors from the data shown in Figure 15. In addition, errors are computed for in-

termediate altitudes at 600 km and 1200 km. The reduction in overall errors is evident when compared to the existing inverse coefficients. As the histograms show, the overall error decreases with increasing altitude. It should be pointed out that the tail of the distribution with large errors (>100 km) corresponds to magnetic latitudes below $\sim 30^\circ$ and the majority of errors above this latitude are <10 km in magnitude.

7. Discussion

To this point the accuracy with which the AACGM coefficients, and their inverses, produce the desired coordinates have been analyzed. Both sets of coefficients have been shown to have improved errors over the existing AACGM coefficients. A final comparison is performed in order to determine the extent to which the transformations, using the forward and inverse coefficients, negate each other. For this test conversions from geographic to AACGM and back to geographic coordinates are performed using the AACGM coefficients. Errors are then determined for each geographic grid point as the difference between original and computed coordinates in great circle distance.

Figure 16 shows the resulting errors for a representative year (2000) and at 0 km altitude. Figure 16a and 16b correspond to the process using old and new AACGM coefficients, respectively. In both cases the errors are relatively low (>50 km) with the exception of the longitude sector associated with the SAA; -60° to 60° . In this region elevated errors extend to the poles but with decreasing amplitude. Errors are, in general, larger using the old AACGM coefficients, with the exception of a narrow band in latitude near

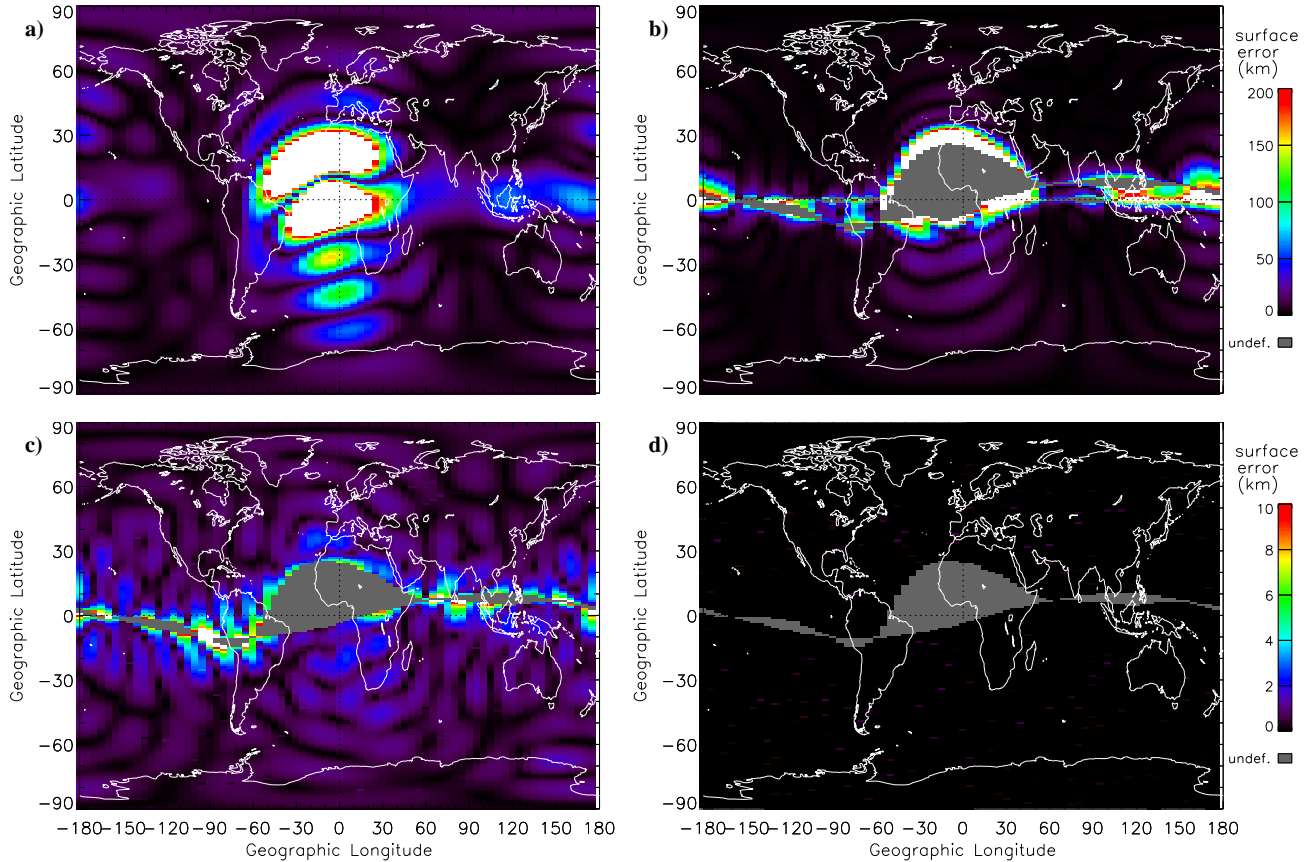


Figure 16. Error associated with conversion from geographic to AACGM and back to geographic coordinates using (a) old and (b) new AACGM coefficients, (c) new AACGM coefficients for the forward transformation and field-line tracing for the inverse, and (d) field-line tracing for both transformations.

the magnetic equator. It is the attempt at reducing the error in this region that appears to be the main focus of the more recent studies. However, increased accuracy in this region has come at the expense of accuracy in the middle to polar latitude regions.

A final comment is that some studies appear to use this type of test to validate the accuracy of the AACGM coefficients. It is important to note that such a test merely confirms the degree of invertibility of the transformation. This author maintains that the coefficients are intended to represent the AACGM coordinates (and their inverse) as accurately as possible and comparisons of results obtained from using the coefficients to those obtained from accurate field-line tracing are more meaningful performance metrics.

Note that while errors are extremely low (<10 km) using the new AACGM coefficients for the forward transformation, they are somewhat unsatisfyingly large for the inverse transformation, particularly below 30° . One alternative for reducing the overall accuracy is to use field-line tracing for the inverse transformation. Figure 16c shows the resulting error when AACGM coefficients are used for the forward transformation (geographic to AACGM) and field-line tracing is used for the inverse (AACGM to geographic.) Note that color scale has been reduced to 10 km in order to reveal errors that are due entirely to the forward transformation.

For situations where the highest degree of accuracy is necessary, field-line tracing in both directions is recommended. Although it is computationally more expensive than evaluating an expansion of spherical harmonic functions, errors associated with field-line tracing are <1 km. Figure 16d shows the errors resulting from performing the coordinate trans-

formation in both directions using field-line tracing, which are <1 km everywhere.

The examples chosen here are for 0 km altitude, where errors are generally largest. Similar behavior is observed over the altitude range 0–2000 km with overall errors decreasing with altitude as the magnetic field becomes more dipolar and the difficulties associated with functional representations of discontinuous data are reduced.

One final point is related to the 5-year period at which IGRF and AACGM coordinates are updated. AACGM coefficient sets have been derived for the 5-year epochs between 1965–2015. For the time period after the latest epoch (2010), secular variations of the IGRF model are used to provide extrapolation for up to another five years beyond this date [Finlay *et al.*, 2010]. A linear interpolation of these coefficients in time between adjacent 5-year epochs has been implemented in the software package developed to exploit the new AACGM coefficients in order to improve fidelity throughout the full epoch range.

Figure 17 shows the AACGM latitude of a single geographic location for each year over the period of 1965–2015. The location chosen is the potential future site of a pair of SuperDARN radar in Graciosa, Azores (39.033° N, 28.036° W). The altitude selected is 600 km, a typical height for the topside ionosphere. While radar backscatter most certainly occurs at higher latitudes than the location of the radar, this location is simply being used as a representative position of interest.

The AACGM coordinates of this location, determined by field-line tracing, are shown in red in Figure 17. The coordinates obtained from the two sets of AACGM coefficients, old and new, are shown in blue and green, respectively. The

existing AACGM software uses only the 5-year epoch coefficients and the AACGM coordinates are, therefore, constant over the duration of each epoch. At this particular location the AACGM latitude is changing at a rate of $\sim 0.1^\circ \text{ yr}^{-1}$, which leads to the possibility of an additional error of $\sim 0.5^\circ$ in latitude over a given 5-year epoch and demonstrates the need for interpolation in time to accurately map coordinates through each epoch.

Figure 17 shows that the new AACGM coefficients do extremely well at reproducing the AACGM coordinates of this location, which is in the SAA sector. The top panel of Figure 17 shows that errors are $< 1 \text{ km}$ in great circle distance for the new AACGM coefficients, while they are $> 10 \text{ km}$ for all but a few years when using the old AACGM coefficients and even exceed 100 km in earlier years. Note that differences in the AACGM longitude also contribute to the overall error that is shown in the top panel. The AACGM latitude is shown in the bottom panel because of its relative importance in organizing ionospheric and magnetospheric processes.

8. Summary

The accuracy to which the current AACGM coefficients produce the actual AACGM coordinates has been investigated. Developments in the technique used to obtain the AACGM coefficients have focused on the equatorial and SAA regions, where the AACGM coordinates are not defined, and on increasing the altitude range over which the coefficients are valid. These developments have led to apparent inconsistencies in the various 5-year epoch sets of AACGM coefficients. Furthermore, emphasis on defining AACGM coordinates with alternative coordinates in regions where they are undefined, the so-called forbidden regions, have led to coefficients that are less accurate in middle to polar regions, where these coordinates were originally intended for use.

Taking the approach that the AACGM coefficients should replicate the AACGM coordinates to the best possible extent, particularly in the middle to polar latitude regions, a new set of AACGM coefficients has been produced for the years 1965–2015. These new coefficients are shown to be a significant improvement over the existing coefficients, with

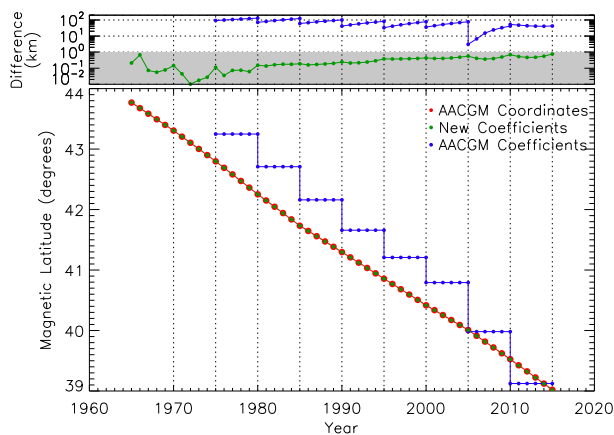


Figure 17. AACGM latitude at 600 km altitude of future SuperDARN radar site located in the Azores. Red indicates the AACGM coordinates determined from the various IGRF models. Blue and green indicate the results using the current and new AACGM coefficients. Linear interpolation in time has been used for the new coefficients. Errors in great circle distance are shown in the top panel for the two sets of coefficients.

errors in great circle distance limited to a few kilometers over most of the globe, with the exception of a band of a few degrees in latitude near forbidden regions. The corresponding AACGM inverse coefficients also show improvement over the existing coefficients, however errors are larger (tens of kilometers) due to the discontinuous nature of the AACGM latitude coordinate near the equator, particularly in the SAA sector.

A software package has been developed for use with these new coefficients. In addition to improved accuracy in the middle to polar latitude region, the ability to use the more accurate, albeit computationally slower, magnetic field-line tracing has been included. It is now possible to limit errors to $\sim 1 \text{ km}$ for transformations to and from geographic and AACGM coordinates.

In order to maintain sufficient accuracy throughout the altitude range that includes LEO, the altitude range over which the new coefficients are valid is limited to 0–2000 km. Above this altitude, field-line tracing can be used for transformation between coordinates.

A simple linear interpolation between coefficients that are defined at 5-year intervals has been implemented. The interpolation scheme eliminates additional errors associated with the 5-year update interval and leads to coordinates varying smoothly in time over the entire time-period for which AACGM coordinates are now defined: 1965–2015.

It is the intent of this work to provide a more transparent, consistent and accurate description of AACGM coordinates and the limitations associated with various functional approximations used in their representation. The new coefficients and software package provide a means for more accurate determination of AACGM coordinates, and their inverse, leading to more consistent mappings in the near-Earth space environment. Coefficients, software, and future updates are made available at <http://engineering.dartmouth.edu/superdarn/aacgm.html> and as supporting information.

Acknowledgments. This work was made possible by continued support of the NSF; grant ATM-0838356. The author gratefully acknowledges Haje Korth for use of the IDL Geopack DLM software, and Mike Ruohoniemi and members of the Virginia Tech SuperDARN group for valuable discussions related to AACGM coordinates.

Larry Kepko thanks Haje Korth and another reviewer for their assistance in evaluating the paper.

References

- Baker, K. B., and S. Wing (1989), A new coordinate system for conjugate studies at high latitudes, *J. Geophys. Res.*, *94*(A7), 9139, doi:10.1029/JA094iA07p09139.
- Bhavnani, K. H., and C. A. Hein (1994), An improved algorithm for computing altitude dependent corrected geomagnetic coordinates, *Tech. Rep. PL-TR-94-2310*, Phillips Lab., Geophys. Dir., Hanscom Air Force Base, Mass.
- Cousins, E. D. P., and S. G. Shepherd (2010), A dynamical model of high-latitude convection derived from SuperDARN plasma drift measurements, *J. Geophys. Res.*, *115*(A12329), doi:10.1029/2010JA016017.
- Doe, R. A., M. Mendillo, J. F. Vickrey, L. J. Zanetti, and R. W. Eastes (1993), Observations of nightside auroral cavities, *J. Geophys. Res.*, *98*(A1), 293, doi:10.1029/92JA02004.
- Finlay, C. C., S. Maus, C. D. Beggan, T. N. Bondar, A. Chambodut, T. A. Chernova, A. Chulliat, V. P. Golovkov, B. Hamilton, M. Hamoudi, R. Holme, G. Hulot, W. Kuang, B. Langlais, V. Lesur, F. J. Lowes, H. Luehr, S. Macmillan, M. Mandea, S. McLean, C. Manoj, M. Menvielle, I. Michaelis, N. Olsen, J. Rauberg, M. Rother, T. J. Sabaka, A. Tangborn, L. Toffner-Clausen, E. Thebault, A. W. P. Thomson, I. Wardinski, Z. Wei, T. I. Zvereva, and I. A. G. A. Wo (2010), International geomagnetic reference field: the eleventh generation, *Geophys. J. Int.*, *183*(3), 1216, doi:10.1111/j.1365-246X.2010.04804.x.

- Greenwald, R. A., K. B. Baker, J. M. Ruohoniemi, J. R. Dudeney, M. Pinnock, N. Mattin, J. M. Leonard, and R. P. Lepping (1990), Simultaneous observations of dynamic variations in high-latitude dayside convection due to changes in IMF B_y , *J. Geophys. Res.*, *95*(A6), 8057, doi:10.1029/JA095iA06p08057.
- Gustafsson, G. (1984), Corrected geomagnetic coordinates for epoch 1980, in *Magnetospheric Currents*, edited by P. Potemra, *Geophys. Monogr. Ser.*, vol. 28, p. 276, AGU, Washington, D. C.
- Gustafsson, G., N. E. Papitashvili, and V. O. Papitashvili (1992), A revised corrected geomagnetic coordinate system for epochs 1985 and 1990, *J. Atmos. Terr. Phys.*, *54*, 1609.
- Hanuse, C., C. Senior, J.-C. Cerisier, J.-P. Villain, R. A. Greenwald, J. M. Ruohoniemi, and K. B. Baker (1993), Instantaneous mapping of high-latitude convection with coherent HF radars, *J. Geophys. Res.*, *98*(A10), 17,387, doi:10.1029/93JA00813.
- Hein, C. A., and K. H. Bhavnani (1996), An expanded altitude algorithm for computing altitude-dependent corrected geomagnetic coordinates, *Tech. Rep. PL-TR-96-2274*, Phillips Lab., Geophys. Dir., Hanscom Air Force Base, Mass.
- Heres, W., and N. A. Bonito (2007), An alternative method of computing altitude adjustment corrected geomagnetic coordinates as applied to IGRF epoch 2005, *Tech. Rep. AFRL-RV-HA-TR-2007-1190*, Air Force Res. Lab., Space Vehicles Dir., Hanscom Air Force Base, Mass.
- Korth, H., B. J. Anderson, and C. L. Waters (2010), Statistical analysis of the dependence of large-scale Birkeland currents on solar wind parameters, *Ann. Geophysicae*, *28*(2), 515.
- Lühr, H., A. Aylward, S. C. Bucher, A. Pajunpaa, T. Holmboe, and S. M. Zalewski (1998), Westward moving dynamic sub-storm features observed with the IMAGE magnetometer network and other ground-based instruments, *Ann. Geophysicae-Atmos. and Space Sci.*, *16*(4), 425-440, doi:10.1007/s00585-998-0425-y.
- Newell, P. T., S. Wind, C.-I. Meng, and V. Sigillito (1991a), The auroral oval position, structure, and intensity of precipitation from 1984 onward - an automated online data-base, *J. Geophys. Res.*, *96*(A4), 5877, doi:10.1029/90JA02450.
- Newell, P. T., W. J. Burke, E. R. Sanchez, C.-I. Meng, M. E. Greenspan, and C. R. Clauer (1991b), The low-latitude boundary-layer and the boundary plasma sheet at low altitude - prenoon precipitation regions and convection reversal boundaries, *J. Geophys. Res.*, *96*(A12), 21,013, doi:10.1029/91JA01818.
- Rodger, A. S., M. Pinnock, J. R. Dudeney, K. B. Baker, and R. A. Greenwald (1994), A new mechanism for polar patch formation, *J. Geophys. Res.*, *99*(A4), 6425, doi:10.1029/93JA01501.
- Rosenberg, T. J., Z. Wang, A. S. Rodger, J. R. Dudeney, and K. B. Baker (1993), Imaging riometer and HF radar measurements of drifting F-region electron density structures in the polar-cap, *J. Geophys. Res.*, *98*(A5), 7757, doi:10.1029/92JA02550.
- Rostoker, G., J. C. Samson, F. Creutzberg, T. J. Hughes, D. R. McDiarmid, A. G. McNamara, A. V. Jones, D. D. Wallis, and L. L. Cogger (1995), CANOPUS - A ground-based instrument array for remote sensing the high latitude ionosphere during the ISTP/GGS program, *Space Sci. Rev.*, *71*, 743, doi:10.1007/BF00751349.
- Ruohoniemi, J. M., and K. B. Baker (1998), Large-scale imaging of high-latitude convection with Super Dual Auroral Radar Network HF radar observations, *J. Geophys. Res.*, *103*, 20,797.
- Ruohoniemi, J. M., R. A. Greenwald, K. B. Baker, and J. C. Samson (1991), HF radar observations of Pc5 field line resonances in the midnight/early morning MLT sector, *J. Geophys. Res.*, *96*(A9), 15,697, doi:10.1029/91JA00795.
- Samson, J. C., R. A. Greenwald, J. M. Ruohoniemi, T. J. Hughes, and D. D. Wallis (1991), magnetometer and radar observations of magnetohydrodynamic cavity modes in the Earth's magnetosphere, *Can. J. Phys.*, *69*(8-9), 929.
- Samson, J. C., B. G. Harrold, J. M. Ruohoniemi, R. A. Greenwald, and A. D. M. Walker (1992), Field line resonances associated with MHD wave-guides in the magnetosphere, *Geophys. Res. Lett.*, *19*(5), 441, doi:10.1029/92GL00116.
- Sotirelis, T., P. T. Newell, and C.-I. Meng (1998), Shape of the open-closed boundary of the polar cap as determined from observations of precipitating particles by up to four DMSP satellites, *J. Geophys. Res.*, *103*(A1), 399, doi:10.1029/97JA02437.
- Watanabe, M., T. Iijima, M. Nakagawa, T. A. Potemra, L. J. Zanetti, S. Ohtani, and P. T. Newell (1998), Field-aligned current systems in the magnetospheric ground state, *J. Geophys. Res.*, *103*(A4), 6853, doi:10.1029/97JA03086.
- Waters, C. L., B. J. Anderson, and K. Liou (2001), Estimation of global field aligned currents using the Iridium (R) System magnetometer data, *Geophys. Res. Lett.*, *28*(11), 2165, doi:10.1029/2000GL012725.

Corresponding author: S. G. Shepherd, Thayer School of Engineering, Dartmouth College, 14 Engineering Dr., Hanover, NH 03755, USA. (simon.g.shepherd@dartmouth.edu)